ON ANISOTROPY OF SOLAR HARD X-RAY EMISSION

G. PIZZICHINI, A. SPIZZICHINO, and G. R. VESPIGNANI
Lab. TESRE–CNR, Bologna, Italy

(Received 9 February; in revised form 29 October, 1973)

Abstract. A number of solar X-ray events above 10 keV and 20 keV were compiled in order to test for evidence of anisotropic emission. The results are not definite, although the two samples show apparently different behaviours.

Among the mechanism of X-ray emission from solar bursts and of related phenomena, like for instance Compton X-ray scattering, some are in principle apt to introduce a dependence of intensity on the direction of observation. This in turn could be evidenced by a centre-to-limb modulation on the number of events detected at different heliographic longitudes (HL).

It was once pointed out by Ohki (1969) that the frequency of detection of hard X-ray ($h\nu \gtrsim 10$ keV) solar bursts appeared to decrease from the centre to the limb of the solar disk. On the other hand, a maximum of detection frequency around 40–50 deg HL was claimed by Pintér (1969), closing in towards 20–30 deg at 1–10 keV and near the centre at 0.6–1.5 keV. This pattern seemed in agreement with a Takakura-Kai flare model.

We attempt here to reconsider the matter with a larger compilation of events above 10 keV, and a sample above 20 keV. In the $\gtrsim 10$ keV band, the OGO-1 and OGO-3 Atlases of X-ray bursts (Arnoldy *et al.*, 1968; Kane and Winckler, 1969) were examined, covering the period from 5 Sept. 1964 to 31 Dec. 1967. Fourteen events from OGO-5 were collected among those reported by Kane (1969) and by Kane and Anderson (1970). In the $\gtrsim 20$ keV band, the events were selected from the list of 'pre-OGO' measurements reported by Arnoldy *et al.* (1968), from the list of OSO-3 events which McKenzie (1971) labelled 'Channel 4' ($\gtrsim 20$ keV), and from the events given by Brini *et al.* (1973) from the Bologna experiment on OSO-6.

A comprehensive list of all the events considered is given in Tables I and II. The heliographic locations are based as usual on associations with Hα flares reported in *Solar-Geophysical Data*, subject to the condition that no other flares be reported with end time later than, or start time earlier than the time of X-ray maximum. Exceptions were made when the overlapping flares occurred at approximately the same HL, whereby no serious ambiguity should arise within the context of this procedure. The X-ray time of maximum for the OGO-1 and -3 events was deduced with an accuracy of typically one minute from the profile time scales on the Atlases.

The events were distributed in 10 deg bins of HL by splitting in two halves the contributions of those falling at exact multiples of 10 deg, except for including all events at 90 deg in the 80–90 deg bin (Figure 1).

Solar Physics **35** (1974) 431–439.

TABLE I

⩾ 20 keV X-ray bursts with associated flares

Date		X-ray max. UT	Flare max. UT	Flare locat.	Imp.
Prior to OGO (Arnoldy *et al.*, 1968; Ohki, 1971)					
1958	20 Mar	1305	> 1330	N25E28	2
1959	31 Aug	2253	2252	S08W46	2+
	1 Sep	1700	1700	S12W53	2+
1960	11 Aug	1929	1928	N22E27	3+
	12 Oct	1731	1728	S16W60	1
	12 Oct	1747	1750	N11W24	1
1961	20 Jul	1553	–	S05W90	3
	28 Sep	2217	2222	N13E30	3
1962	17 Mar	1940	1940	S10E90	1–
	13 Apr	0849	0850	N10E79	1+
	19 Apr	1936	1937	N08W11	2
	21 Apr	0204	0203	N07W26	1+
	1 May	0649	–	N19W68	1
OSO-3 (McKenzie, 1971)					
1967	23 Mar	2238.4	2239	N23E42	1–
	28 Mar	0703.4	0704	N22W14	1
	30 Mar	1941.6	1940	N21W55	1
	31 Mar	1710.4	1712	N18W62	1–
	9 Apr	1755.4	1755	S23W42	–N
	19 May	1505.2	1505	N24E68	–N
	20 May	2211.4	2209	N22E46	–N
	22 May	0116.0	0115	N25E47	–N
	22 May	0151.6	0152	N24E53	–B
	24 May	1427.8	1426	N26E17	–N
	25 May	0130.5	0135	N30E14	–N
	25 May	2051.6	2055	N26E06	1N
	27 May	2314.0	2314	N16W05	–N
	2 Jun	1636.0	1641	N24E22	–N
	2 Jun	2101.9	2101	N22W50	–N
	16 Jun	0411.8	0411	S17W90	1N
	23 Jun	1907.9	1901	N18E23	1B
	23 Jul	2116.0	2116	N23E54	–N
	24 Jul	0323.1	0307–0327	N25E51	1N
	25 Jul	0400.3	0354–0406	N28E44	2F
	25 Jul	1305.2	1307	N28E39	–N
	26 Jul	1305.5	1306	N27E27	–N
	27 Jul	1121.9	1117	N25E13	1N

Table I (continued)

Date		X-ray max. UT	Flare max. UT	Flare locat.	Imp.
	27 Jul	1408.5	1403	N27E14	– N
	28 Jul	1620.4	1623	N30E00	– N
	29 Jul	2243.9	2246	N27W26	– N
	30 Jul	1052.6	1051	N13W07	1N
	31 Jul	1120.8	1120	S25E38	1B
	5 Aug	1810.6	1810	N21E55	– B
	19 Aug	2157.8	2159	N14E67	– N
	26 Aug	2110.6	2111	N14W06	1N
	27 Aug	0023.6	0025	N24W12	– B
	27 Aug	1648.1	1648	N13W18	– N
	29 Aug	0218.9	0220	S22W40	– N
	27 Oct	1942.6	1945	S21E87	– F
	10 Nov	1529.6	1530	S27W84	1F
	16 Nov	1329.6	1334	N09E38	– F
	19 Nov	0511.2	0512	N08E03	– B
	28 Nov	0325.0	0328	N23W53	– N
	30 Nov	2056.8	2058	S30W65	– F
	1 Dec	1459.3	1457	S28W80	– N
	20 Dec	1254.3	1254	N18W44	– N
	22 Dec	1434.8	1434	N20W75	– F
	26 Dec	0046.9	0048	S20E86	– N
1968	12 Jan	0208.8	0208	N20E14	– N
	29 Jan	2222.8	2221	N10E05	– B
	30 Jan	2245.3	2245	N15W05	– F
OSO-6 (Brini *et al.*, 1973)					
1969	4 Nov	0409	0410	N22E79	1B
	4 Nov	0414	0414	N08E89	1N
	21 Nov	2134	2135	N08W03	2B
	21 Nov	2310	2311	N06W10	2B
	22 Nov	2125	2131	N10W14	2B
	23 Nov	0241	0244	N07W25	1B
	26 Nov	1711	1710	N14W68	– N
	27 Nov	1527	1530	S16E44	– B
	30 Nov	1707	1710	N23E02	– N
	16 Dec	0757	0759	N15E36	– N
	26 Dec	0243	0243	S23W05	– B
1970	23 Mar	1547	1548	N18W62	1N
	24 Mar	0923	0925	N16W75	1B
	25 Mar	1220	1226	N14E10	1B
	29 Mar	0056	0046	N13W37	2B
	31 Mar	1807	1813	S12E45	2B

TABLE II

⩾ 10 keV X-ray bursts with associated flares

Date		X-ray max. UT	Flare max. UT	Flare locat.	Imp.
OGO-1 and 3 (Arnoldy *et al.*, 1968)					
1965	2 May	0048	0051	N28E78	1 −
	21 May	2340	2343	N23W11	1 −
	5 Jun	1813	> 1835	S09W49	1 −
	30 Sep	1937	1939	N21E30	2
	2 Oct	1619	1622	N19E05	1
1966	16 Mar	1629	1628	N15E60	SB
	16 Mar	1922	1923	N16E55	1B
			1917	N36W56	SF
	18 Mar	0425	0427	N16E39	SF
	18 Mar	0442	0445	N15E41	1B
	19 Mar	1401	1402	N21E27	SB
	20 Mar	0224	0234	N20E20	1N
	20 Mar	1803	1805	N21E12	1N
	20 Mar	1900	1859	N20E09	1B
	24 Mar	0238	0238	N22W42	2B
	30 Mar	1250	1249	N27E47	2N
	31 Mar	1902	1906	N30E36	1N
	1 Apr	1752	1800	N29E21	1N
	4 Apr	0734	0745	N27W08	2N
	15 Apr	1008	1010	N18E40	2N
	4 May	0154	0153	N29W67	1B
	5 Jul	2022	2019	N33W33	− B
	6 Jul	1303	1305	N34W40	− N
	6 Jul	2030	2032	N33W45	1F
	6 Jul	2150	2152	N34W46	− N
	6 Jul	2225	2230	N34W46	− N
	7 Jul	0038	0043	N34W48	2B
	10 Jul	1632	1632	N19W44	− F
	12 Jul	1152	1157	N25E90	− N
	23 Jul	0241	0243	N38E40	− B
	23 Jul	0550	0552	N37E36	1B
	28 Aug	1528	1529	N23E04	3B
	20 Sep	0826	0828	N22E19	1 +
	13 Oct	0432	0432	N21E66	2
	14 Oct	0531	0530	N21E50	1 −
	14 Oct	1308	1309	N21E42	2 −
	15 Oct	1921	1925	N21E25	1 +
	17 Oct	0247	0247	N22E09	1
	17 Oct	0431	0429	N22E05	2 +
	20 Oct	2042	2043	N12E65	1 −
	23 Oct	1024	1024	N13E25	1 −
	23 Oct	1425	1428	N14W76	1
	23 Oct	2103	2108	N14W80	1
	23 Oct	2355	2356	N14E17	1
	22 Nov	1840	1837	N32W20	1 −
	9 Dec	0307	0307	N23E59	1 −
	9 Dec	1800	1806	N22E50	2

Table II (continued)

Date		X-ray max. UT	Flare max. UT	Flare locat.	Imp.
	10 Dec	1743	1747	S24E08	1
	11 Dec	0545	0542	N18E77	1 –
	11 Dec	1919	1920	S20W09	1
	21 Dec	1942	1945	N20E90	1 –
	23 Dec	0239	0232	N20E74	1 –
	23 Dec	0800	0810	N23E77	1
	23 Dec	1114	1115	S27E73	1
	23 Dec	1312	1312	N21E79	1
	23 Dec	1506	1509	N21E71	1
OGO-1 and 3 (Kane and Winckler, 1969)					
1967	14 Jan	1306	1307	N14W37	1 –
	4 Mar	1716	1717	N24W68	1 +
	23 Mar	1930	1933	N24E35	2 –
	27 Mar	2127	2129	N24W24	1
	1 Apr	0617	0621	N19W71	1B
	1 Apr	0836	0837	N19W74	1B
	1 Apr	1413	1410–1424	N20W79	1B
	11 Apr	1123	1124	S21W65	1N
	6 May	0441	0437	S21W35	3N
	10 May	1206	1211	S20W85	1N
	21 May	1540	1539	N23E57	1B
	23 May	1840	1845	N27E25	2B
	23 May	1940	1955	N27E28	2B
	28 May	0550	0546	N28W33	3B
	18 Jun	0121	0123	N26E63	2B
	23 Jun	0048	0050	N15E34	1N
	16 Jul	$<$ 2342	2350	S18E90	– N
	22 Jul	1655	1655	N28E80	– N
	23 Jul	1300	1301	N12E76	1B
	24 Jul	0035	0036	N11E66	1N
	24 Jul	0929	0933	N27E54	1N
	24 Jul	1001	1000	N10E64	1B
	25 Jul	1056	1058	N26E39	– N
	25 Jul	1213	1216	N27E40	1N
	25 Jul	1625	1628	N28E37	– N
	25 Jul	1644	1647	N16E45	– F
	25 Jul	2100	2101	N28E36	1N
	25 Jul	2252	2255	N22E37	– N
	26 Jul	0226	0231	N27E33	1N
	26 Jul	0656	0701	N26E30	1B
	26 Jul	1806	1805	N14E30	– N
	27 Jul	0511	0518	N27E17	– N
	27 Jul	1737	1736	N29E13	1N
	28 Jul	0011	0014	N29E09	1N
	31 Jul	1503	1514	N25W47	– N
	31 Jul	1723	1724	N13W21	– N
	1 Aug	0642	0642	N24W55	1N
	1 Aug	1608	1612	N20E07	– N
			1611	N13W09	– N

Table II (continued)

Date		X-ray max. UT	Flare max. UT	Flare locat.	Imp.
	3 Aug	0929	0927	N26W82	1N
	9 Aug	1633	1632	N27W69	– B
	3 Aug	1827	1829	S24E32	2B
	6 Aug	1447	1446	S24E78	1N
	12 Aug	1609	1609	S24W05	2B
	17 Aug	2103	2106	N09W13	1B
	18 Aug	2130	2138	N25E91	1N
	19 Aug	0006	0005	N18E83	2N
	19 Aug	1612	1608	N13E74	– N
	19 Aug	1741	1749	N13W66	– N
	20 Aug	1612	1614	N18E67	1N
	20 Aug	2026	2031	N24E62	– N
	21 Aug	1839	1844	N23E49	2N
	27 Aug	0102	0103	N22W12	– N
	28 Aug	1214	1212	S21W30	1B
	29 Aug	1800	1801	S21W52	– N
	29 Aug	1944	1950	N22W50	1B
	29 Aug	2052	2054	N22W50	1B
	31 Aug	2150	2150	N23W81	– N
	12 Sep	1354	1355	N24W61	– N
	6 Oct	1223	1224	S17W37	1N
	22 Oct	1011	1010	N11E23	1B
	22 Oct	2215	2217	N10E14	1B
	29 Oct	0305	0301	N09W80	1N
	2 Nov	0858	0859	S18W02	1B
	10 Nov	0858	0855	S27W72	– N
	27 Nov	1608	1610	N24W54	1F
	2 Dec	0543	0546	S27W87	1F
	22 Dec	0542	0547	N23W65	1N
	24 Dec	1940–1950	1942	S29W23	– N
OGO-5 (Kane, 1969)					
1968	19 Apr	1610.2	1612	N20W61	– F
	3 Jul	2329.2	2330	N26W80	– B
OGO-5 (Kane and Anderson, 1970)					
1968	13 Apr	1009.8	1013	N26E18	– N
	16 Apr	2248.3	–	N22W24	– B
	30 Apr	0518.6	0519	N20E73	– B
	3 May	2226.0	2227	N21E20	– N
	10 May	1904.6	1905	N20W77	N
	22 May	1828.4	1830	N19E04	– B
	24 May	1254.5	1255	N24W22	– N
	25 May	1652.5	1654	N23W38	– N
	28 May	0554.9	0555	N24W72	1B
	15 Jun	2334.5	2333	S13W30	– B
	20 Jun	0707.0	0709	N14E05	– N
	26 Jun	0511.7	0514	N14W68	– B

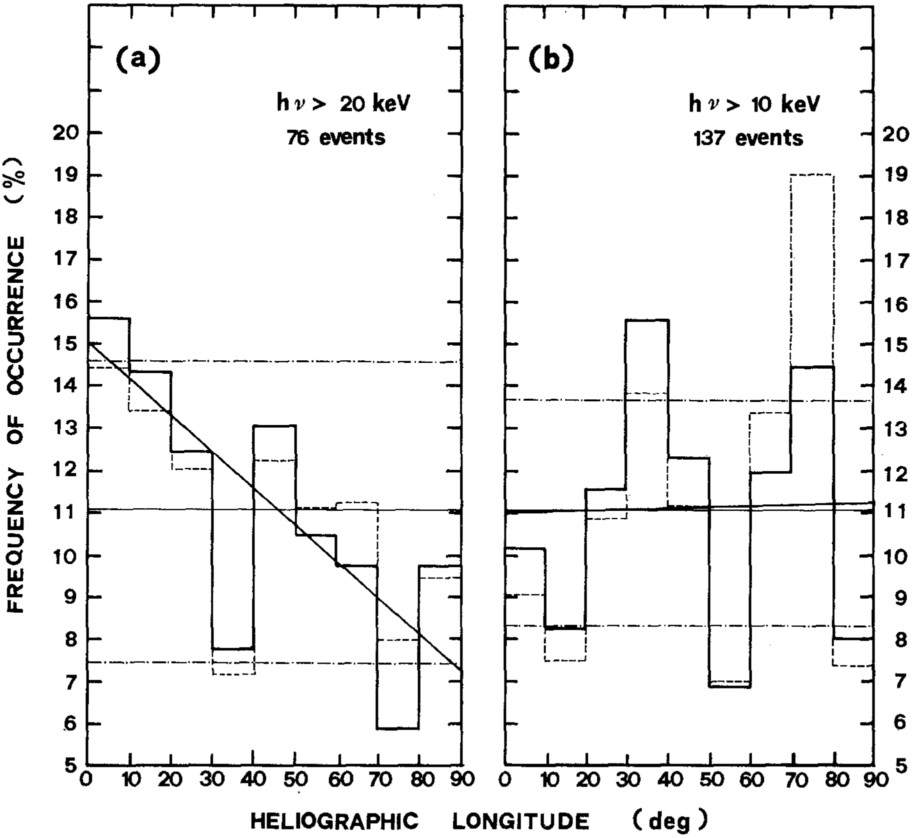

Fig. 1. Normalized distributions of $\gtrsim 20$ keV and $\gtrsim 10$ keV X-ray solar bursts according to the heliographic longitude of associated Hα flares (solid lines). The distribution after correction for Hα visibility is in broken lines. The horizontal straight lines indicate the average and corresponding 3σ levels. The linear best fits are also indicated.

An 'Hα correction' has been deduced from the HL distribution of flares given by Drake (1971), as a possible correction for the Hα visibility effect. This correction is applied by dividing each number of observed X-ray events in a 10 deg interval by the corresponding value of the Hα flare distribution. This procedure should roughly compensate for the Hα visibility distribution being folded onto the X-ray bursts distribution through the process of X-ray to Hα association. The resulting corrected values are drawn in dotted lines in Figure 1, but they have not been adopted for this exploratory analysis.

A quantitative estimate of possible features of the uncorrected distribution n (HL) has been made by χ^2-testing the goodness of fit to a constant level given by their average m over the 0–90 deg HL range, to a linear best fit, and to a Poisson distribution $m^n e^{-m}/n!$. The latter fit amounts to testing the randomness of the numbers of events observed with a 10 deg 'window', but otherwise irrespective of their HL

TABLE III

χ^2 tests and significance levels $F_n(\%)$ with n degrees of freedom for fits to HL distributions

Fit \ Sample		(a) $\gtrsim 20$ keV	(b) $\gtrsim 10$ keV
const $= m$	χ^2	5.5	8.8
	F_8	70	35
linear best fit	χ^2	2.6	8.8
	F_7	95	25
Poisson (mean $= m$)	χ^2	9.3	5.5
	F_8	35	70
m		8.4	15.2

location, about a mean corresponding to their observed average over the whole disk. However, the significance of this test is very low, since only 9 'observations', and with poor statistics, are given to evaluate a mean and to fit a Poisson curve.

Table III summarizes the results of these tests on the two samples, for nine HL bins 10 deg wide. From a simple statistical point of view, the significance of the samples is still such that it matters how one defines the angular bins, but if we take the results at their face value, one consideration can be made. It appears that the first sample ($\gtrsim 20$ keV) would have a poor fit to the hypothesis of randomness but a fair probability of fitting a non-zero slope. The second sample ($\gtrsim 10$ keV) would not fit well a hypothesis of linearity, while exhibiting a peak $> 3\sigma$ above the average, between 30 and 40 deg. This happens to be near that of Pintèr whose sample of 46 events is included in the present one.

Discussion

The obvious requirement of a better statistical resolution is only one of the conditions necessary to definite results. Since the effects of anisotropic emission should depend on the emission mechanism, on source configuration and on energy distribution, it is likely that uncharacteristic compilations such as these show no definite features or lead to incorrect conclusions anyhow.

In order to obtain physical information on solar X-ray emission through possible signature of directivity, which is the aim of this kind of search, many different samples will have to be collected distinctly, depending on such parameters as, in a first instance, the sensitivity threshold of detection, the classification of events in 'impulsive' and 'gradual' bursts, in 'thermal', 'quasi-thermal' or 'non-thermal', and, even then, their spectral hardness.

If, however, the indications given by these samples were to be confirmed, a peak of visibility should be moving towards the centre from 10 keV to 20 keV. In a simple minded view this could mean that energetic bursts arose from upward-moving streams of electrons rather than from Takakura-Kai configurations.

On the other hand, not only could the emitted spectrum depend on direction, as in the case of non-thermal Bremsstrahlung, but it might also be significantly altered by secondary processes depending on direction of observation and on photon energy. One such process is the multiple Compton scattering of hard photons emitted towards the solar surface, resulting in a backscattered component at present indistinguishable from the primary emission. Quantitative estimates of spectral distortion as a function of angle of observation have been made by Santangelo *et al.* (1973) in the hard X-ray band. Their results show how even an isotropic emission could give rise to an anisotropic total flux of hard X-rays (primary backscattered) with a strong ($\approx 30\%$) enhancement towards the centre of the disk.

Aside from external factors, the effects arising just within the source can be expected to be complex and not always univocal. For example, the computations of Elwert and Haug (1971) on the directivity of non-thermal Bremsstrahlung emission show clearly how widely the result can be changed by diffeıent details in the electrons spectrum and their pitch angles in the magnetic field.

Finally, the effect of an assumed directivity of emission can be translated with some reliability into a modulation of the *number* of observed events when the sample comes from consistent observations with the same detection threshold and depending on the parameters assumed to define a 'luminosity function' of a class of X-ray bursts. An approximate relation between intensity modulation and number modulation was indicatively examined by Brini *et al.* (1973).

Acknowledgements

We wish to thank Dr S. R. Kane and Prof. J. R. Winckler for providing us with the OGO-1 and OGO-3 Atlases. We are also grateful to our referee whose initial comments helped in the revision of this paper.

References

Arnoldy, R. L., Kane, S. R., and Winckler, J. R.: 1968, *Astrophys. J.* **151**, 711; and 1968, CR-108, Univ. of Minnesota.
Brini, D., Evangelisti, F., Fuligni Di Grande, M. T., Pizzichini, G., Spizzichino, A., and Vespignani, G. R.: 1973, *Astron. Astrophys.* **25**, 17.
Drake, J. F.: 1971, *Solar Phys.* **16**, 152.
Elwert, G. and Haug, E.: 1971, *Solar Phys.* **20**, 413.
Kane, S. R.: 1969, *Astrophys. J.* **157**, L139.
Kane, S. R. and Anderson, K. A.: 1970, *Astrophys. J.* **162**, 1003.
Kane, S. R. and Winckler, J. R.: 1969, CR-134, Univ. of Minnesota
McKenzie, D. L.: 1971, Thesis, UCSD SP 71-03.
Ohki, K. I.: 1969, *Solar Phys.* **7**, 260.
Pintér, S.: 1969, *Solar Phys.* **8**, 142.
Santangelo, N., Horstman, H., and Horstman-Moretti, E.: 1973, *Solar Phys.* **29**, 143.
Solar-Geophysical Data – ESSA Reports, Boulder.